

Increased coastal wave hazard generated by differential wind and wave direction in hyper-tidal estuaries



Charlotte E. Lyddon^{a,b,*}, Jennifer M. Brown^b, Nicoletta Leonardi^a, Andrew J. Plater^a

^a University of Liverpool, School of Environmental Sciences, Liverpool, L69 7ZT, United Kingdom

^b National Oceanography Centre Liverpool, Joseph Proudman Building, 6 Brownlow Street, Liverpool, Merseyside, L3 5DA, United Kingdom

ARTICLE INFO

Keywords:

Delft3D
Estuarine dynamics
Hyper-tidal
Coastal wave hazard
Wave propagation
Wind wave properties

ABSTRACT

Wave overtopping and subsequent coastal flood hazard is strongly controlled by wind and water levels, and is especially critical in hyper-tidal estuaries where even small changes in wave heights can be catastrophic if they are concurrent with high spring tide. Wave hazard in estuaries is largely attributed to high amplitude shorter period, locally generated wind waves; while low amplitude longer period waves rarely impact low-lying coastal zones up-estuary. Here, the effect of wind and wave properties on up-estuary wave propagation and the sensitivity of significant wave height are investigated numerically along the shoreline of the Severn Estuary, southwest England, as an example. Representative values for wind speed and direction, wave height, period and direction are used to identify key combinations of factors that define the wave hazard generation. High amplitude, short period wind waves are sensitive to opposing winds, with a steepening effect that varies along the estuary shoreline, highlighting the effect of estuarine geometry on wave hazard. Low amplitude, long period wind waves respond with maximum variability in significant wave height to strong winds resulting in their propagation further up-estuary. Our results advance current understanding of the compound interaction between wind and waves, and identify critical conditions maximizing the hazard and hazard variability along the shoreline. The outcomes from this research can help to avoid economic losses from operational downtime in ports and harbors, inform sustainable coastal sea defense design and understand how wave hazard may vary under future climate due to changing storm tracks. Results can also be applied to the design of coastal infrastructure and facilitation of emergency response planning.

1. Introduction

1.1. Wave hazard impacts

The coincidence of waves with spring high tide and strong winds with a long fetch can be catastrophic in heavily populated and industrialized hyper-tidal estuaries (Desplanque and Mossman, 1999; Wolf, 2009). The highest waves superimposed on high water levels can cause an instantaneous uprush of water at the coast and push large volumes of water over seawalls or dikes in a short period of time (Hoeke et al., 2015; EurOtop, 2016). This has implications for run-up, wave overtopping, spray and subsequent coastal flooding, which is critical for users and property along the coastline (Allsop et al., 2008; Wolf, 2008; Bastidas et al., 2016; Thompson et al., 2017). Mean overtopping discharges exceeding 0.03 l/s per m, as a function of wave height, wave steepness and water depth (Allsop et al., 2005; Burcharth and Hughes, 2011) can pose a hazard to public safety (EurOtop, 2016). Despite many

seawalls designed to withstand this threshold, 4–8 people are killed each year in the UK through the direct effects of waves on seawalls (Allsop et al., 2005) and approximately 60 killed in Italy over the last 20 years (Allsop et al., 2003).

Wave overtopping imposes serious hazard in heavily populated and industrialized estuaries, where infrastructure, transport networks and natural resources may be located (Geeraerts et al., 2007). Coastal harbors located in hyper-tidal estuaries are economic hubs in terms of trade, communication and tourism. For instance, the Royal Portbury Docks in the Severn Estuary are important for shipping and distribution, and supports 10,000 jobs (Bristol Port Company, 2018). The Port of Shanghai on the Yangtze Estuary is the busiest container port in the world facilitating one of the fastest growing coastal economies (Yap and Lam, 2013). Liverpool Docks in the Mersey Estuary, northwest England, support cruise ships, ferries and vessels which maintain and develop a large network of offshore windfarms (Peel Ports, 2018). Coastal ports and harbors must maintain operating conditions throughout the year,

* Corresponding author. University of Liverpool, School of Environmental Sciences, Liverpool, L69 7ZT, United Kingdom.

E-mail address: C.E.Lyddon@liverpool.ac.uk (C.E. Lyddon).

<https://doi.org/10.1016/j.ecss.2019.02.042>

Received 2 August 2018; Received in revised form 8 February 2019; Accepted 18 February 2019

Available online 04 March 2019

0272-7714/ Crown Copyright © 2019 Published by Elsevier Ltd. This is an open access article under the CC BY license (<http://creativecommons.org/licenses/by/4.0/>).

even during extreme conditions, to minimize economic risks and risks to humans and their property (Santana-Ceballos et al., 2017).

Ports and critical infrastructure are often located in estuaries because they are sheltered by land from the impacts of high-energy waves and wind conditions (Phillips, 2008; Uncles, 2010). It is assumed that up-estuary locations are subject only to the effects of high amplitude, shorter period, locally generated wind waves (Lesser, 2009), tides, river flow and storm surges (Monbaliu et al., 2014). However it cannot be assumed that large, hyper-tidal estuaries display a uniform response to forcing factors to provide shelter at all times (Allen and Duffy, 1998), and in some instances estuary orientation can act to amplify wave hazard up-estuary (Grady and McInnes, 2010). Longer period waves could generate a significant and underestimated hazard up-estuary if exacerbated by local wind-wave effects (Talke and Stacey, 2003), due to their relatively high run-up compared to higher amplitude waves (Palmer et al., 2014). The largest overtopping waves, generated under stronger winds on younger sea states in the estuary, can plunge into water in the lee of seawalls, harbors walls and breakwaters and cause new waves to be formed (EurOtop, 2016). New waves in ports and harbors, known as transmission waves, can excite harbor seiche and cause unnecessary back-and-forth motions of vessels and subsequent risk for safety thresholds, including avoiding vessels coming loose from moorings (Donger et al., 2016).

Run-up will increase with increasing wavelength and wave period (EurOtop, 2016), therefore assuming the influence of longer period waves is negligible in estuaries can present a hazard if defenses are not designed to protect against them. This paper will explore how coastal wave hazard changes through a large, hyper-tidal estuary under varying wind wave conditions, to provide an understanding of the frequency, pattern and severity of wave overtopping events. Better understanding of the sensitivity of coastal wave hazard to the interaction of local wind and waves enables more informed decisions by managers of critical coastal infrastructure responsible for operational flood risk management and implementation of policies, which may vary in time, over a 100-year management horizon.

1.2. Wave hazard in hyper-tidal estuaries

Coastal zones worldwide are subject to local changes in water level due to the combined effect of astronomical high tides, waves and wind (Allsop et al., 2008; Letchford and Zachry, 2009; Bastidas et al., 2016). Strong winds blowing over the surface of shallow water generate waves which propagate towards the coast at a speed and amplitude dependent on water depth (Wolf, 2009). Coastal wave hazard can cause danger to life and property when coinciding with stronger wind speeds (Wolf, 2009) or around the time of high water. This is of particular significance in hyper-tidal estuaries where the tidal range exceeds 6 m and where even small changes in total water levels and wave setup can be catastrophic if occurring during high tide (Davies, 1964; Robins et al., 2016).

Large tidal ranges occur as a consequence of the orientation, geometry and bathymetry of the estuary funneling and amplifying tidal wave propagation (Pye and Blott, 2014). Extreme water depths, due to a large tidal range, allow waves to propagate far up-estuary, with the impact of waves felt along large stretches of coastline (Brown and Davies, 2010; Brown et al., 2010). The Bay of Fundy, Canada, which has a tidal range over 16 m (Desplanque and Mossman, 1999), could in some respects be described as a wave-dominated coast due to the long fetch creating locally-generated waves (Davis and Hayes, 1984). High amplitude storm waves can also develop in the Bay due to strong, prevailing southeasterly to southwesterly winds (Desplanque and Mossman, 2004). Severe flood conditions are “virtually guaranteed” in the Bay of Fundy when strong winds and adverse weather conditions coincide with high water of large, astronomical tides (Desplanque and Mossman, 2004). Measurements of significant wave height in the lower Bay at Tyner Point show that waves exceed 1 m from November to April

25% of the time, and are characterized as swell waves with a period longer than 9 s and locally-generated waves with a 5 s period (Greenberg, 1984). Severe storms, such as the “Groundhog Day” storm of 1976 can produce longer period waves (Greenberg et al., 2012). The Severn Estuary, south-west England, is a long shallow, narrow estuary which creates mean spring tidal range up to 12.2 m at Avonmouth (Pye and Blott, 2010). The incidence and strength of incoming south-westerly-westerly storms from the Atlantic, tidal modulation and current fields have a strong control on wave evolution up-estuary (Allen and Duffy, 1998). A combination of strong winds and a tidal bore caused wave overtopping in Minsterworth, Maisemore, Elmore and Newnham in the Severn Estuary on 3–4 January 2014, causing flooding of roads and houses (BBC, 2014; Haigh et al., 2015). Waves approaching the estuary from 200 to 250° (Sibley et al., 2015) were followed by maximum 25 m/s (55 mph) wind from 230° (CEDA, 2018). Sea defenses were overtopped by water levels up to 0.8 m above crest height, with £2.8 million damage to Welsh sea defenses (as documented in SurgeWatch (Haigh et al., 2015)). Under certain conditions, wind-waves could propagate up-estuary and potentially overtop sea defenses at Barry (7.39 m AOD/12.89 m CD) or Penarth (8.53 m AOD/14.3 m CD) (Welsh Office, 1999). Rougher wind-wave seas are unlikely to overtop concrete sea walls at Hinkley Point as their crest height exceeds 8.5 m AOD (14.4 m CD) (Magnox, 2014). However, the Bristol Channel is only affected by a narrow band of storm tracks, which means there is only a 50% chance of a severe storm, and maximum wave height, coinciding with high water (Dhoop and Mason, 2018), which can make waves less significant in terms of flooding (Fairley et al., 2014). The orientation of an estuary can also shelter it from swell waves, as seen in the Mersey Estuary, northwest England which predominantly experiences locally wind-generated waves (Wolf, 2008). The largest waves in Liverpool Bay, which can exceed 4 m during 1–5 storm events per year, are generated by westerly-northwesterly winds which have the longest fetch (Brown and Wolf, 2009). Locally generated, high amplitude waves can still affect infrastructure and utilities, as seen in the Dee Estuary on 5 December 2013. The railway line was closed from Holyhead to Chester as gale force winds caused damage to the line at Colwyn Bay (Natural Resources Wales, 2014). Wave amplitude is critical in overtopping hazard thresholds for setting safety margins for people, property and transport (EurOtop, 2016).

Simulations of Tropical Cyclone Agnes, August 25, 1981 and Matsa, July 21, 2005, in Hangzhou Bay, where mean spring tidal range can exceed 8.1 m (Zhang et al., 2012), shows wave overtopping can occur in the estuary regardless of wind direction when wind speed is strong enough. Easterly winds with a wind speed of 40.7 m/s (90 mph) were recorded during Tropical Cyclone Matsa, which affected 31.5 million people in the region (Hu et al., 2007; Zhang et al., 2012). Due to the size and hydrodynamics in hyper-tidal estuaries, it cannot always be assumed that ports and infrastructure located up-estuary are sheltered from the effects of swell wave hazard. Wave overtopping volumes and impacts will be site specific, and closely related to the local bathymetry and topography, size and use of the receiving area (Allsop et al., 2008) and characteristics of sea defense structures (Santana-Ceballos et al., 2017). New observations (Brown et al., 2018) at the mouth of the Mersey, NW England, found wave overtopping alerts need to have an increased consideration for the offshore wave conditions. An event with a NW wind caused overtopping along a seawall frontage 26th October 2017, while no alert was triggered due to the wind direction not being directly onshore and the wave conditions being considered as relatively low amplitude. The duration, fetch and strength of wind, in addition to water depth, sheltering effects due to estuary orientation and geometry are important controls on wave evolution and propagation in an estuary.

Accurate prediction of nearshore waves is essential in heavily populated and industrialized estuaries for coastal wave and flood hazard mitigation. Accurate forecasts of coastal waves and understanding of the potential impact is critical for the accurate provision of conditions

at the coastal boundary of flood hazard models (of overtopping or inundation) used to inform management activities (Prime et al., 2016) or within operational flood forecast systems (Bocquet et al., 2009). Such prediction requires an accurate understanding of wave generation and evolution at high water combined with the effect of wind, wave type and fetch. Analysis and prediction of wave hazard can improve understanding of the processes and contributions to maximum significant wave heights and economic impacts of waves at the coast. Modeling approaches are often employed to simulate wave generation and evolution to assess the potential consequences of wave overtopping at tidal high water, and subsequent coastal flood hazard for people, businesses, and the natural and built environment. A coupled wave circulation model application to Mobile Bay, Alabama during Hurricane Georges (1998) in the Gulf of Mexico (Chen et al., 2007) shows spatial and temporal variability of wave heights and wave periods. The results can be applied to the design of coastal infrastructure and facilitation of hurricane emergency planning. There is a clear economic case for improved prediction of nearshore waves during storm events as the replacement cost of sea defenses around England has been estimated at £6 billion (\$8 billion USD) (Allsop et al., 2005). However, simulation of wave hazard in a hyper-tidal estuary is complex due to the extreme tidal range, complex geometry and bathymetry and random nature of wind-generated waves (Santana-Ceballos et al., 2017). Prediction of maximum significant wave heights at high water can facilitate the management and emergency response of coastal resources, improve the design of sea defenses and coastal infrastructure to reduce economic risks, and inform the public and decision makers to minimize loss of life from extreme wave events.

1.3. Case study

This research focuses on the Severn Estuary, south-west England, as a test case of hyper-tidal estuaries worldwide, due to its national significant for nuclear and energy assets and because it has the second largest tidal range in the world. For the purposes of this paper the “Severn Estuary” is taken to include the Bristol Channel. The Severn Estuary has a mean spring tidal range of up to 12.2 m at Avonmouth, due to near-resonance and tidal amplification as a result of the funneling effect (Dyer, 1995; Uncles, 2010; Lyddon et al., 2018a,b). The width of the mouth of the Severn Estuary, up to 41 km between Woolacombe, Devon and Rhossili, Gower Peninsula, and the westerly-southwesterly aspect means the estuary is exposed to prevailing southwesterly winds with a long fetch and ocean waves from the North Atlantic (Pye and Blott, 2010). Observational wave data from the directional waverider buoy at Scarweather, 15 km off the coast of Porthcawl, South Wales, between 1 January 2012 and 31 December 2016 show on average waves approach from a WSW to W direction (245.4°) (Fig. 1). The waves have an average significant wave height of 4.8 m, average wave period of 8.3 s and peak period up to 22.2 s. Swell waves enter the estuary from the Atlantic Ocean and can generate a bimodal wave regime, particularly under stormy conditions (Proctor and Flather, 1989). Waves approaching from a SW/W have the longest fetch, indicating wind waves generated along longer local fetches can reach longer periods.

This paper describes the effect of wind and wave properties on spatial variability and sensitivity of significant wave height along the shoreline of a hyper-tidal estuary. A sensitivity study is conducted using representative values for wave height, period and direction and wind speed and direction to force the model boundary of Delft3D-WAVE. As explained in the method (Section 2), waves are simulated on a spring tide to explore the relative significance of high amplitude, shorter period wind generated waves compared with low amplitude, longer period waves. The results (Section 3) identify key combinations of factors which are important for exacerbating wave hazard in ports, harbors and towns and sheltering effects along the shoreline. Before drawing conclusions in Section 5 we discuss in section 4 the

significance of wave hazard that can be exacerbated by local wind-wave effects in hyper-tidal estuaries, where tide and surge are often considered the primary hazard.

2. Methods

2.1. Delft3D-wave

Delft3D is a modeling suite which is used to simulate flows, waves and morphological developments for coastal, river and estuarine environments (Lesser et al., 2004). Delft3D-WAVE, a third generation spectral wave model, simulates the evolution of wind-generated waves over time and space (Delft Hydraulics, 2014). Delft3D-WAVE is based on the SWAN model (Simulating WAVes Nearshore (Booij et al., 1999)), which is designed to simulate short-crested waves in shallow, coastal regions dependent on wind forcing, water depth and bottom roughness. The physical processes simulated by Delft3D-WAVE include wave generation by wind, dissipation due to whitecapping, depth-induced wave breaking, bottom friction (using the JONSWAP formulation) and refraction (Delft Hydraulics, 2014). The modeling system has been successfully applied to many coastal and estuarine regions (Elias et al., 2012; Bastidas et al., 2016).

A 2DH, curvilinear model grid is used to simulate nearshore waves in the Severn Estuary, SW England using Delft3D-WAVE. The model grid extends from Woolacombe, Devon and Rhossili, South Wales in the west to Gloucester in the east and follows the shape of the coastline (Fig. 2). The model grid resolution has been refined at the coast to improve the accuracy of significant wave height prediction along the shoreline, as this is the area of most interest in this study. Gridded bathymetry, data at 50 m resolution (SeaZone Solutions Ltd. 2013) was interpolated over the 2DH curvilinear grid by grid-cell averaging and triangular interpolation. The wave model is forced at one open boundary to the west, with representative water level, significant wave height, wave period and wind speed values.

2.2. Boundary conditions

A schematic diagram of the wave model and forcing data sources used for the model boundary conditions is shown in Fig. 3.

2.2.1. Water level

A large tidal range and strong tidal currents result in tidal modulation of wave conditions in the Severn Estuary (Fairley et al., 2014). For the purpose of this study, which aims to isolate the effect of wind and wave conditions on wave hazard, Delft3D-WAVE is run as a standalone wave model to remove the influence of tidal modulation, wave-current interaction and wind setup on significant wave height. The study aims to build on previous research into tide-surge interaction (Lyddon et al., 2018a, 2018b), prior to assessing the effect of wave hazard on flood inundation. The model's open sea boundary to the west of the model domain (Fig. 2) is forced with a constant water level. This water level is the average of mean high water spring tide at Mumbles (4.54 m) and Ilfracombe (4.47 m) (NTSLF, 2018) to produce representative mean high water spring tide (MHWST) value of 4.5 m (relative to chart datum). MHWST was chosen as a representative water level as wave hazard could be increased when wind waves are superimposed on a higher water level.

2.2.2. Wave selection

Observational wave data, recorded by the WaveNet directional waverider buoy at Scarweather (51°25'.99N, 003°55'.99W, shown in Fig. 2) is analyzed to identify representative wave height and period to force the model boundary (CEFAS, 2018). Five years of significant wave height and average wave period, recorded from 1 January 2012 to 31 December 2016 which occurs when the tide is at or above the level of MHWST, is plotted to separate and isolate representative shorter and

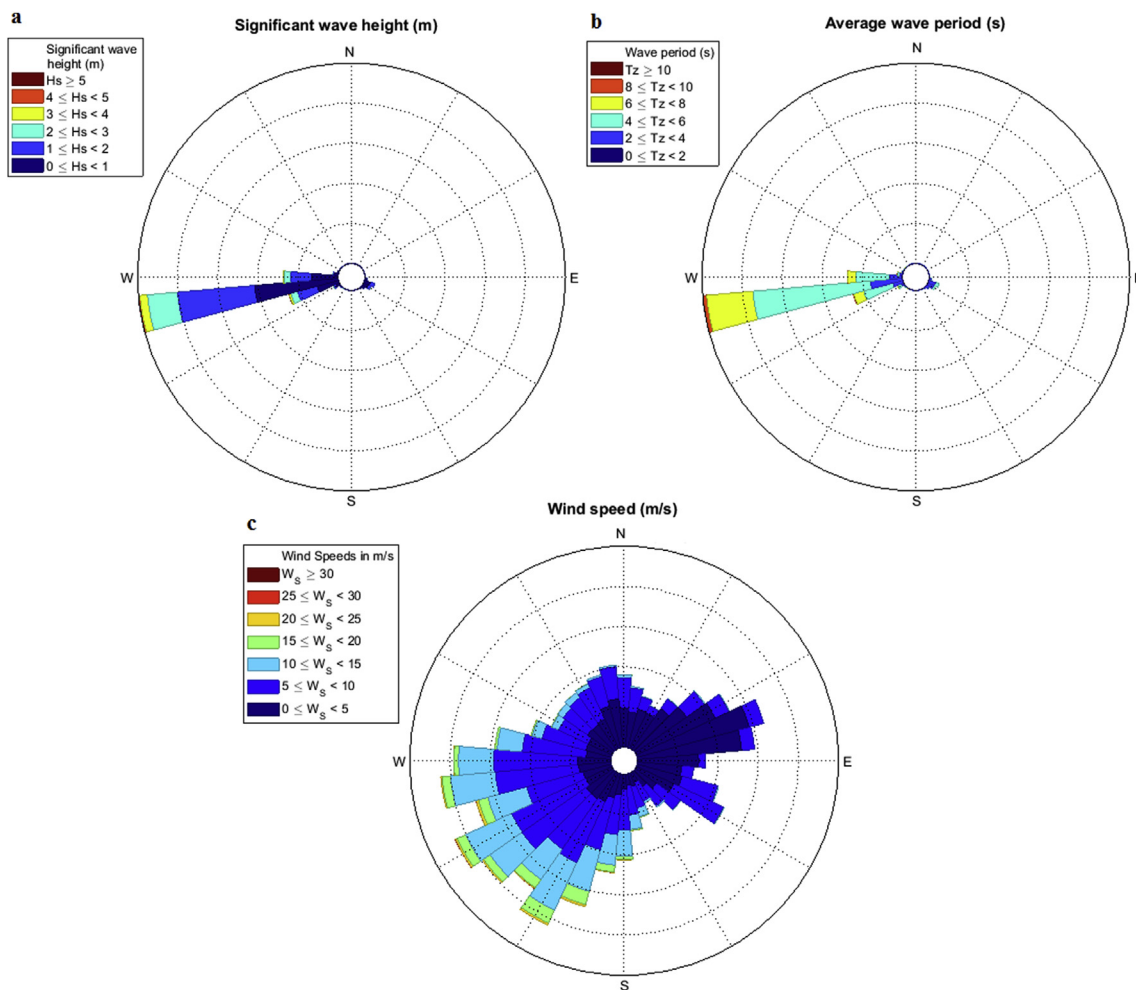


Fig. 1. 5 years of observational wave buoy data taken from Scarweather (located in Fig. 2), Severn Estuary, UK showing a) wave direction (deg) and significant wave height (m), b) average wave direction and wave period (s) and c) 5 years of observational wind data taken from Chivenor, Devon (located in Fig. 2).

longer period wind waves (Fig. 4). The wave record selected provides a series of wave conditions that are representative of conditions which may occur in the estuary, and includes the 2013/2014 winter which

was the stormiest on record (Sibley et al., 2015; Masselink et al., 2016). The record captures low probability, extreme conditions, including the 3 January 2014 storm saw wave heights in excess of 6 m at the

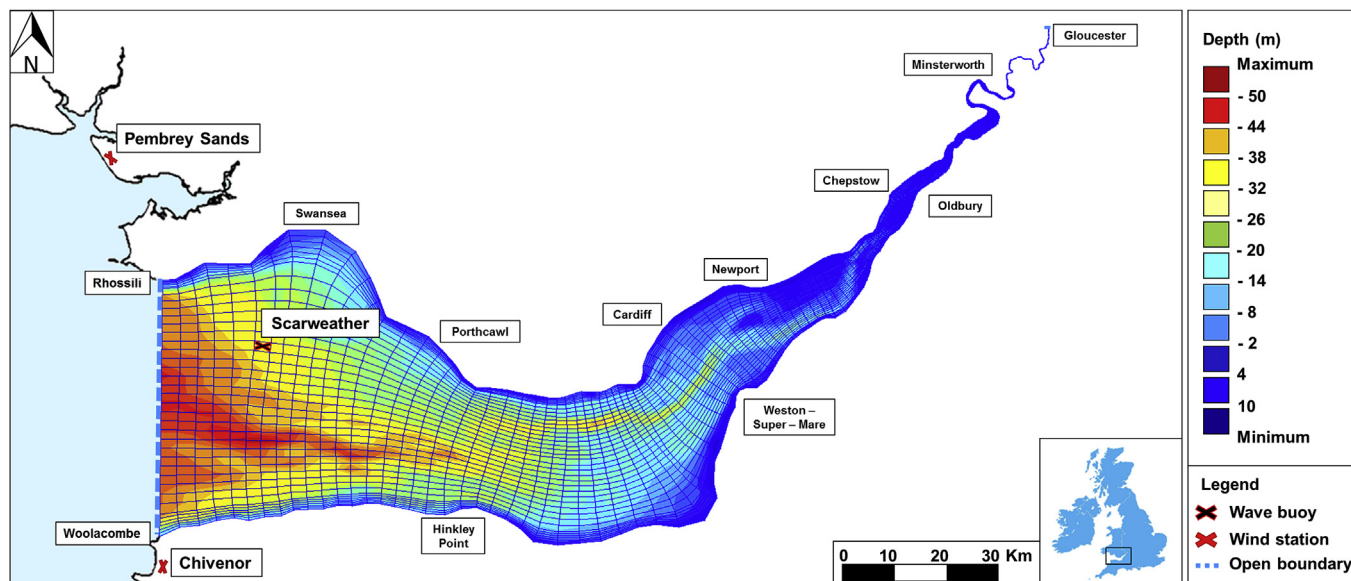


Fig. 2. Deft3D-WAVE model grid. The bathymetry is relative to chart datum (CD).

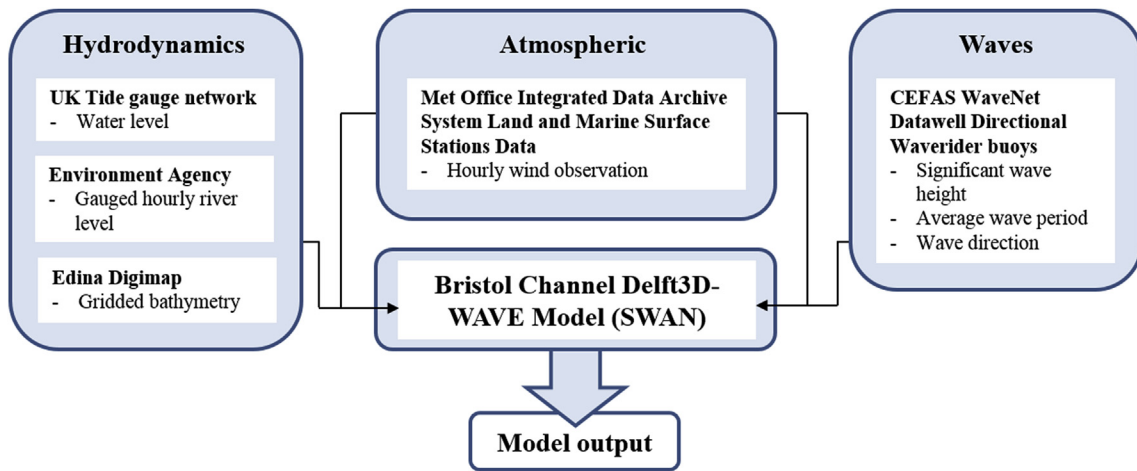


Fig. 3. Model schematic for the coupled Delft3D hydrodynamic (FLOW) and wave (SWAN) model with forcing data sources.

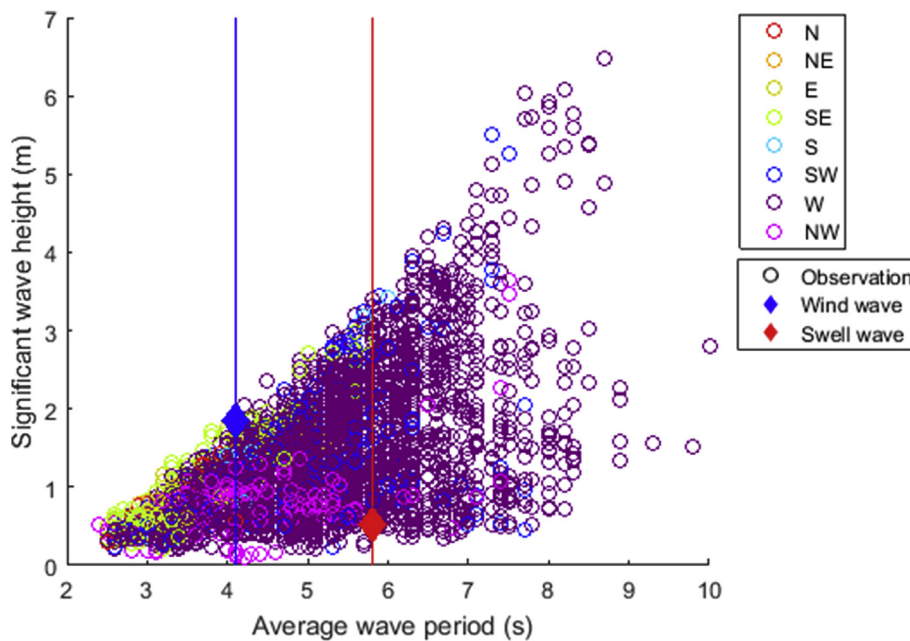


Fig. 4. Wave selection for H_s and T_z . 25th percentile T_z (blue line) and 75th percentile T_z (red line), color coordinated based on wave direction.

Scarweather wave buoy and wave periods up to 20 s (Sibley et al., 2015). As seen in Fig. 4, there is no clear separation between locally generated wind waves and ocean-generated swell waves at or above the level of MHWST. The wave buoy shows a large range of wind waves in response to the range of local fetches NW (fetch limited), W and SW (long fetch open to the Atlantic Ocean). Lower amplitude waves approach from a NW with an average period up to 10 s, and high and low amplitude waves with a range of periods from low to high approach from the W.

Wave parameters typically used for coastal defense design and coastal flooding strategies are average wave period (T_z) and significant wave height (H_s) (Palmer et al., 2014). To isolate representative wave types from the record to force the model boundary, the 25th and 75th percentile values for average wave period are identified, as this parameter relates to wave power and flood hazard (Prime et al., 2016; Thompson et al., 2017). Equivalent significant wave heights are then identified to represent different wave amplitudes, referred to here after as high and low amplitude waves. A higher significant wave height is selected from the observations based at the 25th percentile value for wave period to represent a higher amplitude wave, which is steeper in shape. A lower significant wave height combined with a 75th percentile

value wave period is selected to represent a lower amplitude wave, which is less likely to break at the base which results in water forced upwards and potentially overtopping (Sibley and Cox, 2014). These two wave types have been selected to: compare higher and lower amplitude wave propagation up-estuary; represent wave conditions that could occur in the estuary and potentially result in wave overtopping; and, represent waves that have been documented in hyper-tidal estuaries worldwide (Greenberg, 1984; Wolf et al., 2011). Modeled results of representative values for wave period and significant wave height (Table 1) will show how different waves behave and propagate through the estuary, and the impact of estuary orientation on wave propagation up-estuary. Observations are positioned close to the model boundary

Table 1
Representative wind wave conditions close to the estuary mouth based on 5 years of observational data from Scarweather Waverider buoy.

	H_s (m)	T_z (s)
High amplitude waves	1.86	4.1
Low amplitude waves	0.53	5.8

Table 2

Representative wind speeds based on 5 years of observational data from Chivenor in Devon (England) and Pembrey Sands in Dyfed (Wales) UK Met Office MIDAS land station data.

	Wind speed (m/s)
10 percentile	1.8
50 percentile	5.18
90 percentile	11.06

and thus the two wave conditions (Table 1) are representative of the conditions at the estuary mouth and used to force the open boundary (see Table 2).

The representative wave types presented in Table 1 are combined with varying wave direction (SW, W, and NW) to explore the effect of prevailing wind direction on wave propagation into and through the estuary.

2.2.3. Wind selection

Observational wind data, taken from the UK Met Office MIDAS Land and Marine Surface Station Data located in coastal locations in the outer Severn Estuary at Chivenor and Pembrey Sands (see Fig. 2) are used to define representative wind speeds to force the Delft3D-WAVE model (CEDA, 2018). Five years of wind speed data, recorded from 1 January 2012 to 31 December 2016, are analyzed to identify 10th, 50th, and 90th percentile values for wind speed at each station. The average for each percentile wind speed value is calculated from both coastal stations to provide a spread of representative wind speeds within the estuary. The wind direction is also varied and applied to the model domain from 8 points of the compass (N, NE, E, SE, S, SW, W, and NW). The wind speed and direction is uniform in time and space. This will demonstrate how wave behavior responds to changes in wind speed and direction. Delft3D-WAVE is also run with no wind speed (0 m/s) to provide a baseline scenario and to isolate the effect of wind speed and wind direction on wave hazard.

2.3. Model validation and scenarios

Results from model simulation are compared with 5 years of observational data from the Scarweather WaveNet wave buoy in Severn Estuary. The model represents scenario combinations of wave height and wave period combined with varying wave and wind direction. Observational data from the Scarweather waverider buoy, which occurs when the tide is at or above the level of MHWST, are isolated and H_s and T_z plotted (Fig. 4). Model simulations at the same location in the model domain as the Scarweather wave buoy are plotted over the observational wave data (Fig. 5).

Fig. 5 shows the scenario combinations cover a range of observed conditions. Model simulated waves show good agreement for wind directions from the SE, S and SW. The model overestimates waves approaching from NW, N and NE direction because more extreme winds are not typical for this direction and are causing wave growth over the short fetch (see Fig. 1c). The wave buoy records lower amplitude waves approaching the estuary from these directions, as seen in Figs. 1 and 4. The scenario combinations simulate cases (NW waves) which are unlikely to occur in reality. The model under-predicts maximum wave conditions from a W direction, from which the highest amplitude waves approach WSW (see Fig. 5). As seen in Fig. 4, there is a large number of points that exceed the 75th percentile value, which are dominated by higher amplitude, longer period wind waves approaching from the W. The scenario combinations do not capture the direction-specific higher amplitude, longer period waves which could occur.

Some 150 wind-wave scenarios are modeled to identify key combinations of factors which are important for wave hazard and wind-

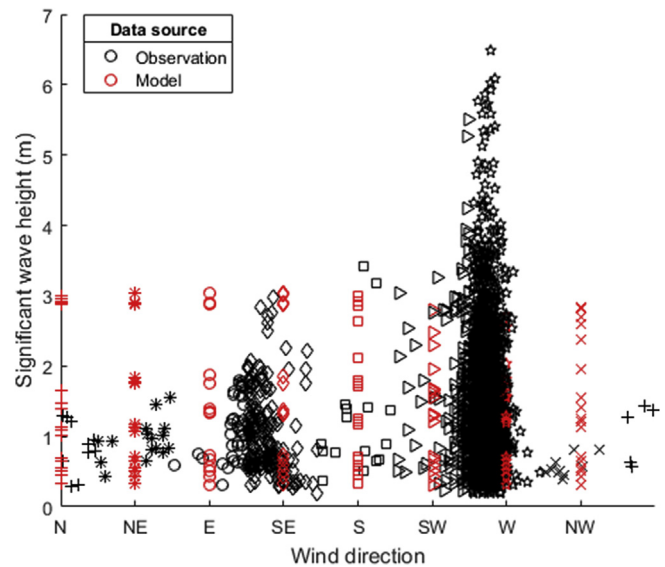


Fig. 5. Delft3D-WAVE model validation comparing model simulations to 5 years observational data at Scarweather wave buoy. Symbols representing directions over a range of 45°.

wave propagation up-estuary. The model domain is forced using a combination of different representative wind and wave conditions, including a baseline scenario for each wave direction and wave type with no wind forcing.

3. Results

Model outputs are analyzed to identify maximum significant wave height every 2 km along the shoreline of the estuary. The difference between the maximum significant wave height along the shoreline and the ‘no wind’ scenario for each wave type and wind direction is presented to quantify the impact of wind on wave hazard. The difference between maximum significant wave height and the baseline scenario is plotted along the shoreline starting at Rhossili, South Wales and moving along the north shoreline of the estuary up to Gloucester, and then along the south shoreline of the estuary to Woolacombe, Devon. Fig. 6a shows the difference between maximum significant wave height and baseline scenario along the shoreline for representative high amplitude waves, and Fig. 6b shows representative low amplitude waves along the shoreline of the estuary. Each subplot in Figs. 6a and 5b represents the wave hazard under a different incoming wave direction, line color denotes the different wind direction and line type denotes different wind speed. Results are presented systematically for the two representative wave types selected.

3.1. High amplitude waves

3.1.1. Maximum significant wave height for high amplitude wind waves

The maximum significant wave height (H_s) produced across all normalized high amplitude wind wave scenarios is 2.04 m, which occurs 20 km up-estuary from the model boundary on the south shoreline. This wave height is produced from a wind wave entering the estuary from a NW direction, with a 90th percentile value wind in an E direction. A 90th percentile value wind speed, 11.06 m/s, represented by the solid lines in Fig. 6a, consistently produces the maximum H_s along each shoreline. As wind speed increases, the friction velocity increases and a steeper, rougher wind sea begins to develop (Lin et al., 2002). There is no consistency along the shoreline as to which wind direction produces the maximum H_s and where this occurs due to the complex orientation of the coastline, however there are a number of general trends which have emerged.

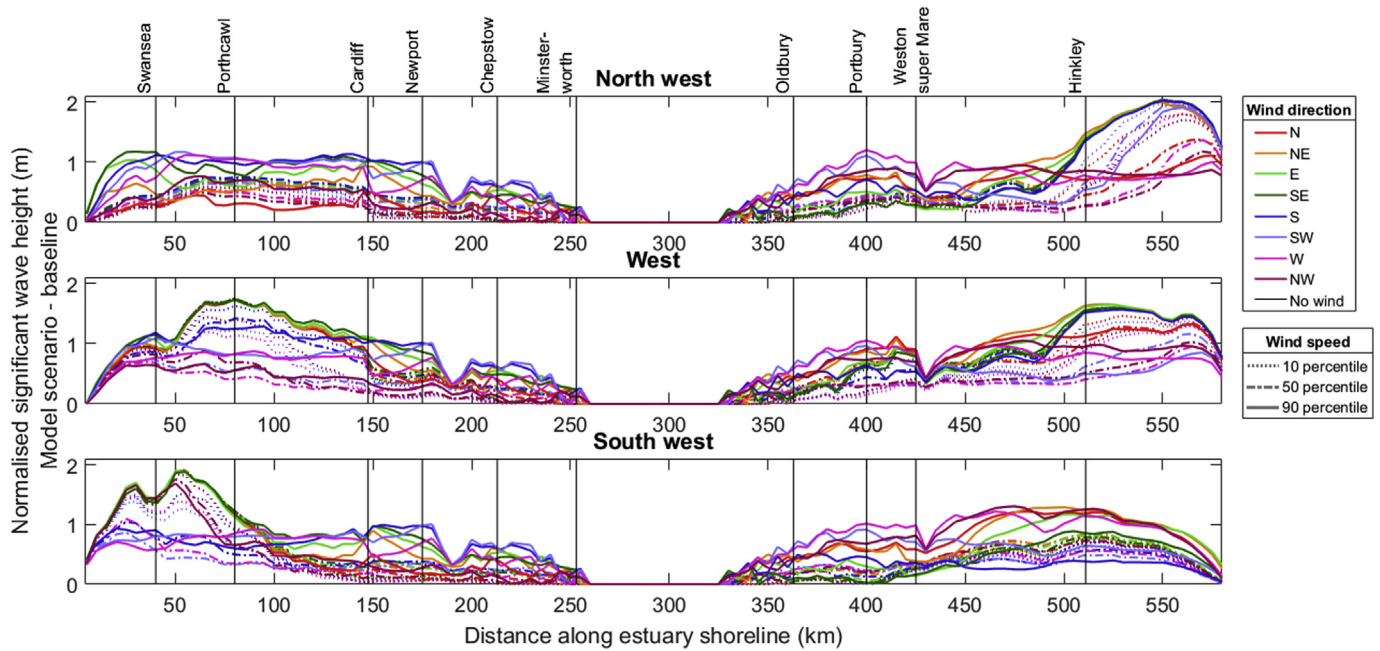


Fig. 6. a) Normalized significant wave height (model scenario – no wind baseline scenario) for representative high amplitude, short period waves along the shoreline of Severn Estuary, starting at Swansea to Gloucester and thence down-estuary towards Hinkley Point. b) Normalized significant wave height (model scenario – no wind baseline scenario) for representative low amplitude, longer period waves along the shoreline of Severn Estuary, starting at Swansea to Gloucester and thence down-estuary towards Hinkley Point.

3.1.2. Following winds reduce Hs in the outer estuary

A high amplitude wind wave moving towards the shoreline with a 90th percentile value wind speed and following wind does not produce the maximum Hs in the outer estuary. For example a wave traveling from the NW followed by a 90th percentile value wind speed produces normalized maximum Hs of 0.79 m, 30 km up-estuary from the model boundary on the south shoreline. A NW wave followed by a 10th percentile value wind speed value produces a normalized maximum Hs of 1.59 m, at the same point in the model domain. Further to this, a wave moving in a SW direction followed by a 90th percentile value wind speed in a SW direction, produces a normalized maximum Hs of 0.84 m

50 km up-estuary from the model boundary on the north shoreline, between Swansea and Porthcawl. A SW wave followed by a 10th percentile wind speed value produces a normalized maximum Hs of 1.23 m at the same point in the model domain. It is evident that a following wind contributes to wave growth. The addition of wind energy to the rougher sea could cause the wave to feel the effect of bottom friction and break before reaching the shoreline or break due to whitecapping.

3.1.3. Opposing, blocking wind acts to steepen waves in the outer estuary

Maximum waves on both south and north shorelines generally occur

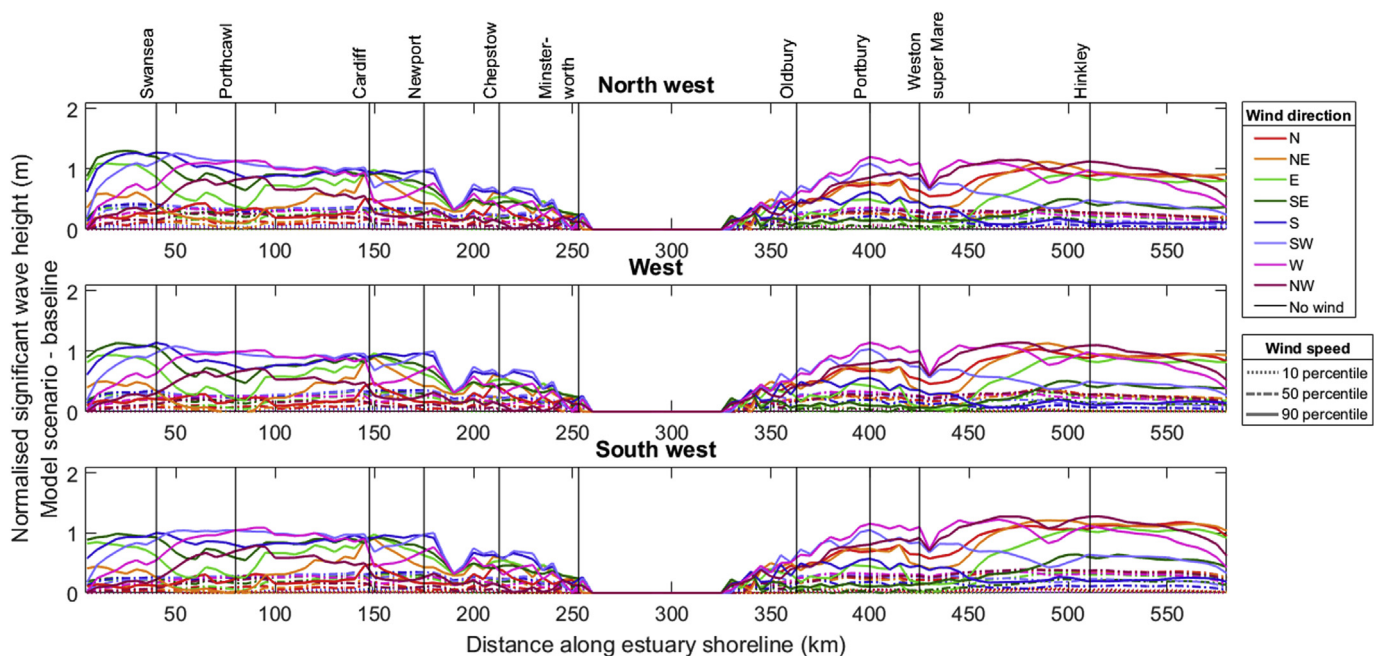


Fig. 6. (continued)

when wind and wave are propagating in opposite directions. For example, the maximum normalized H_s on the south shoreline, 2.04 m, occurs when NW waves are essentially blocked by 90th percentile value wind speed from a SE/E direction. Likewise, the maximum normalized H_s on the north shoreline, 1.91 m, occurs when the SW waves are blocked by 90th percentile value wind speed from a NE/E direction. Winds block the wave propagation moving in the opposite direction to increase the steepness of waves. Further to this, the younger, rougher wind-wave sea shows increased sensitivity to wind direction. This is particularly the case in the outer estuary where there is greater sensitivity to changing wind direction and wind speed. The range of normalized maximum H_s is 1.47 m between Swansea and Porthcawl on the north shoreline and 1.35 m down-estuary of Hinkley Point on the south shoreline. The blocking effect of wind appears to be a significant contribution to wave hazard along the shoreline of the outer estuary.

There is less sensitivity to wind direction in the upper estuary, beyond Cardiff on the north shoreline and Portbury on the south shoreline as waves begin to attenuate. Following winds from the W and SW produce the maximum normalized H_s in the upper estuary, as fetch may help high amplitude waves to propagate further up-estuary. The effect of bottom friction dissipates wave energy and the lines converge to show H_s decline. H_s is 0 m in the upper estuary at Gloucester as wave energy is not able to propagate this far up-estuary, possibly due to the long, narrow, shallow nature of the Severn Estuary.

3.1.4. Effect of estuary geometry on significant wave height

The wind direction produces a different maximum H_s in different locations throughout the estuary, as a function of the local geometry and complex orientation of the coastline. The maximum H_s on the south shoreline occurs with a NW wave direction, and the maximum H_s on the north shoreline occurs with a SW wave direction. It is clear that a shoreline facing an incoming, onshore wave direction will experience increased wave hazard, however the incoming wave direction impacts each shoreline differently. The maximum normalized H_s on the north shoreline occurs further up-estuary, 1.91 m at 55 km away from the model boundary. In contrast, the maximum normalized H_s on the south shoreline, 2.04 m, occurs 30 km up-estuary from the model boundary. The orientation of coast, geometry and bathymetry of the estuary means that the shorelines do not respond in the same way and the maximum is not observed at the same distance up-estuary.

The effect of shoreline geometry on wave hazard is further highlighted by the double peak in maximum significant wave height observed close to Mumbles for a SW wave direction. The headland is smoothed out in the model domain; however complex changes in water depth are reflected in the bathymetry.

3.2. Low amplitude waves

3.2.1. 90 percentile winds create maximum variability

The 90th percentile value wind speed consistently produces the maximum normalized H_s along the north and south shoreline throughout the estuary for longer period, lower amplitude waves (Fig. 6b). Normalized maximum H_s remains steady along the shoreline from the model boundary to Weston-super-Mare on the south shoreline and Cardiff on the north shoreline for each scenario. This shows the wind has a sustained influence in propagating lower amplitude, longer period waves as far up estuary as Chepstow and Oldbury. Further up-estuary the channel begins to narrow and become increasingly shallow, and waves rapidly decay. There is a varying magnitude of normalized maximum H_s for each scenario with a 90th percentile value wind speed. There is over 1 m variability in normalized maximum H_s between scenarios forced by a 90th percentile value wind speed, as opposed to 0.01 m variability for scenarios forced by a 10th percentile value wind speed.

At Porthcawl, on the north shoreline of the estuary, maximum normalized H_s is 1.13 m with a NW wave and a following 90th

percentile value wind speed from a W wind direction. The minimum normalized H_s for a NW wave under a 90th percentile value wind speed is 0.11 m, which occurs with a NE wind. This produces a range of 1.02 m on the north shoreline and shows that lower amplitude, longer period waves can propagate further up-estuary under stronger wind conditions.

In the same location on the north shoreline, normalized maximum H_s under a NW wave direction with a 10th percentile value wind speed is 0.04 m with a SE wind. The lowest normalized H_s produced by a 10th percentile value wind speed is 0 m for a NW wave and E wind. This produces a range of just 0.04 m for H_s at Porthcawl under the 10th percentile value wind speeds. The 0 m normalized H_s at Porthcawl under an E wind shows that the wind is having little effect on significant wave height under this scenario.

The results at Hinkley Point on the south shoreline in the outer estuary follow a similar pattern. The maximum normalized H_s at Hinkley Point is 1.27 m under a SW wave with a 90th percentile value wind speed from the NW. Minimum normalized H_s for a SW wave under a 90th percentile value wind speed is 0.2 m, which occurs with a S wind direction. This produces a range of 1.07 m on the south shoreline of the outer estuary. There is less sensitivity in normalized H_s under 10th percentile value wind speeds. Maximum normalized H_s under a 10th percentile value wind speed for a NW wave is 0.05 m, with a N wind and minimum normalized H_s is 0.01 m, also under a S wind producing a range of 0.04 m. A southerly wind produces the lowest H_s for all percentile value wind speeds, as the orientation of the coastline minimizes the effect of wind to contribute to H_s . Along the north and south shoreline, it is evident that higher period, low amplitude waves show greater sensitivity to wind direction for higher wind speeds.

4. Discussion

The results presented here help to identify the contribution of individual factors to variability in coastal wave hazard in a hyper-tidal estuary. Increased wave hazard along the shoreline may influence wave overtopping, which is an important consideration for port and harbor operations, energy infrastructure and residential communities in estuaries when considering direct flood hazard. The results can also help to understand how wave hazard may vary under future climate change, with varying storm tracks and wind conditions.

4.1. Younger, rougher seas show more sensitivity to wind direction

The model highlights that short period, high amplitude waves are sensitive to wind direction, with a stronger, opposing wind increasing significant wave height. There is known to be a strong coupling and transfer of momentum between turbulent atmospheric and oceanic boundary layers. Increasing wind speed acts to increase the drag coefficient on the sea surface (Pugh, 2004), enhancing generation of wind-waves (Janssen, 1989). The transfer of energy from the atmosphere to sea waves can be affected by sea state (Janssen, 1989). Experimental results show that the drag coefficient over a younger, wind-wave sea is up to 50% larger than an older, swell sea (Donelan, 1982). Further to this, a Boussinesq type wave model has been used to show that wind waves are sensitive to changes in wind speed can amplify significant wave height, due to increased energy exchange between the air and sea (Liu et al., 2015). Stronger winds have been shown to be important in amplifying significant wave height in the Dee Estuary. Simulations of the wind-wave climate of the Dee Estuary under a 1 in 100-year storm under 5, 15 and 25 m/s wind speed show an increase in wave height and setup along the coast, which could contribute significantly to flooding (Wolf, 2007). Changes in the wind speed can alter wave conditions, resulting in local-scale changes in sea level at exposed sites.

The sensitivity of waves to wind direction can be site specific. Opposing winds can cause waves to become shorter and higher, and therefore steeper (Wolf et al., 2011). Steeper waves can cause

unpredictable and unstable sea conditions, as seen in the mouth of the Columbia River when combined with strong, opposing river outflow which can make the region dangerous for shipping and boats (Elias et al., 2012). Strong, opposing winds blowing against incoming low amplitude waves can generate surface waves and tidal rips in the Bay of Fundy, Canada (Desplanque and Mossman, 2004), resulting in dangerous sea conditions. As seen in Fig. 6a, each shoreline can respond differently to prevailing conditions with significant wave height occurring at different distances up-estuary. Simulations of locally wind-generated sea from westerly and northwesterly winds in the Dee Estuary, NW England show that significant wave height varies along the estuary shoreline due to the sheltering effect of West Hoyle Bank and the Welsh coastline and the effect of water depth on refraction (Wolf et al., 2011). Wind direction and speed can act to amplify significant wave height and subsequent wave hazard in hyper-tidal estuaries, and local bathymetry and topography can change influence the response of each shoreline to varying conditions.

4.2. Long period, low amplitude waves amplified due to strong winds

The model confirms that stronger wind speeds are important for increasing H_s for higher period, low amplitude waves throughout the estuary. The drag coefficient of air flow, related to shear stress of wind speed on sea surface, low amplitude, longer period waves, does not respond to the influence of shear stress to the same extent as younger, higher frequency wind waves (Brown and Wolf, 2009). A fully developed wave field, such as a longer period, low amplitude wave, may receive little momentum from the air (Janssen, 1989) and low amplitude waves exhibit less drag than both shoaling and breaking waves (Anctil and Donelan, 1996). The drag coefficient is Delft3D-WAVE is linearly related to wind speed (Wu, 1982), which may account for some of the effect of surface roughness due to wind. Increased variability in significant wave height for stronger wind speeds may be the effect of increasing wind speed on surface roughness and the drag coefficient, generating local winds on the sea surface (Letchford and Zachry, 2009). Long period waves propagate into the Severn Estuary throughout much of the year (Pye and Blott, 2010), and contribute to significant wave heights during low pressure, winter storms (Sibley et al., 2015). Long period waves in the Bay of Fundy, Canada, are exacerbated by strong, southeasterly to southerly winds due to the orientation of the estuary (Desplanque and Mossman, 1999). Strong southerly winds during the Saxby Gale, 4 October 1989 resulted in significant damage, as dykes breached, cattle and sheep drowned and railroad beds washed away and only when the wind shifted to a southwesterly direction did the waves cease to cause damage (Desplanque and Mossman, 2004). However, certain areas in large estuaries can be sheltered from the effect of swell waves due to sheltering, e.g. in the Dee Estuary, NW England (Brown and Wolf, 2009), or shallow water effects which cause extensive dispersion, as seen in San Francisco Bay (Talke and Stacey, 2003). The model has shown that low amplitude, long period waves can propagate far up-estuary which disproves the assumption that up-estuary locations are only subject to storm surges and higher amplitude, locally generated wind waves (Lesser, 2009; Monbaliu et al., 2014). The effect of low amplitude waves may create similar impacts as an energetic swell wave, which has a longer wavelength and lower frequency, to increase wave hazard along the shoreline (Palmer et al., 2014; Sibley et al., 2015). Further to this, stronger wind speeds superimpose locally generated waves on the sea surface, which can result in dangerous sea conditions for critical infrastructure, ports and harbors. Coastal defenses in hyper-tidal estuaries must be designed to protect against the effect of long period, low amplitude wind-waves as well as tides, storm surges and river flow.

4.3. Waves impact on flood hazard and economic activities

The results presented here show the effect of wind and wave

properties on variability of significant wave height along the shoreline of the estuary and can be used as an evidence base to inform future coastal management decisions. Increased significant wave height under certain wind-wave conditions can pose a hazard in coastal areas due to wave run-up and defense overtopping (Bastidas et al., 2016) as individual waves exceed the available ‘freeboard’ (height above still water level) of coastal defenses (Wolf, 2009). The results can be applied to understand the wind-wave condition which could result in maximum significant wave height and subsequent wave overtopping in ports and harbors, which can influence the safety of structures and of people working and traveling immediately behind the defense line (Bouma et al., 2009; Diab et al., 2017). Low amplitudes waves, which can generate rough sea states under stronger winds in the estuary, can propagate into ports and harbors and cause excessive moored ship motions with consequences for operational downtime (Rosa-Santos and Taveira-Pinto, 2013). Operational downtime has financial implications, as cargo handling cannot occur and the ship has to leave berth due to unsafe mooring conditions (Van Deyzen et al., 2015). Knowledge of the wind-wave conditions that can cause wave overtopping, transmission or swell wave propagation in the harbor can be used to divert ships away from port during hazardous conditions, to avoid damage to mooring lines or downtime. The hazards of wave overtopping are site specific, especially when people are concerned, and dependent on estuary orientation, bathymetry and topography (Santana-Ceballos et al., 2017), characteristics of sea walls (Allsop et al., 2005) and the complex nature of wind-generated waves. Increased wavelength and wave period, as seen with swell waves, can also contribute to overtopping hazard as run-up is longer (Thompson et al., 2017), and should also be considered as a hazard in some estuaries. Understanding wave overtopping hazard from combined wind-wave effects can help to reduce economic losses from storm events in estuaries by avoiding operational downtime and damage to vessels and moorings.

The results presented here identify key combinations of wind-wave properties which contribute to wave hazard in a hyper-tidal estuary. While waves contribute towards total coastal water level by means of wave run-up, wave setup and swash (Stockdon et al., 2006; Wolf, 2009), the effect of astronomical tides, atmospheric storm surges and river discharges must also be considered. Wave characteristics and propagation in shallow water is partially dependent on tidal elevation. Wave heights may also be related to surge magnitude, and wind has an important role in generating surge and waves (Pye and Blott, 2014). Tidal modulation of waves plays a large part of the natural regime of the Severn Estuary (Fairley et al., 2014) and strong currents in the Bay of Fundy can generate tidal rips and hazardous surface waves (Desplanque and Mossman, 1999). Future simulations of wind-wave conditions should include tide-surge propagation, evidently important in a hyper-tidal estuary, and the effect of wave hazard sensitivity on morphological response (Phillips et al., 2017), overtopping volumes, and depth and extent of subsequent flood inundation (Prime et al., 2015).

4.4. Changing future storm tracks and climate

The model results can also help to understand how wave hazard may develop under future, changing climate patterns, and the impact this may have on future flood inundation and adaptation strategies. It has been seen that maximum significant wave height varies within the estuary dependent on wind speed and wind direction, therefore stronger wind speeds and changing storm tracks under future climate could alter future flood risk from wave overtopping (EurOtop, 2016). Changes in the number, frequency and track of mid-latitude (30–60°) storm tracks would alter wind speed and direction, which would directly influence wave hazard in estuaries (Robins et al., 2016). Simulations of typhoon intensification in the Pearl Estuary has been shown to increase significant wave height, and results have been fed into design of seawalls (Yin et al., 2017). Increasing sea levels and river

discharge will allow waves to propagate and impact further up-estuary, and are more likely to overtop sea defenses (Wolf, 2007). Increasing frequency and magnitude of storms, or those occurring in clusters, will increase the occurrence of economic damage and potential loss of life across a larger spatial area (Robins et al., 2016). Further to this, changes in storminess have the potential to reduce the effectiveness of existing coastal defenses and result in more extensive and damaging floods (Phillips, 2008). Large scale atmospheric changes, such as the North Atlantic and Southern Oscillations, could also result in changes in wind speed and direction, which will have implications for where maximum significant wave heights will occur, with potential implications in the Severn Estuary and Bay of Fundy (Phillips et al., 2013). However wave hazard under future climate will vary depending on regional- and local-scale processes, strong natural variability and uncertainty in anthropogenic forcing and future wave climate (Woolf and Wolf, 2013; Haigh and Nicholls, 2017). Regional-scale simulations of wind-wave conditions in an estuarine system can identify important processes and interactions which may be effected under future climate. The methodology and results presented here can aid long-term coastal defense and management strategies, as sustainable coastal management requires confidence in the knowledge of any possible future changes to wave hazard.

5. Conclusion

There is a need to identify key combinations of wind-wave characteristics which contribute to wave hazard and the relative significance of wind-generated waves compared with swell waves in heavily populated and industrialized hyper-tidal estuaries, where critical infrastructure must be designed to withstand this hazard. Delft3D-WAVE is used to simulate wave evolution in a hyper-tidal estuary to identify key combinations of wind-wave characteristics which contribute to maximum significant wave height, and subsequent wave hazard throughout the estuary. Long-term wind and wave records are used to generate representative wind-wave conditions, and consider the influence of wind speed, wind direction, wave type and wave direction on maximum significant wave height along the shoreline of the Severn Estuary, SW England. Results show that a younger, rougher wind-wave sea, characterized by low period, high amplitude waves, show increased sensitivity to wind direction. Stronger, opposing winds generate maximum significant wave height in the outer estuary. Maximum significant wave height occurs at different locations up-estuary along each shoreline due to estuary orientation and local bathymetric effects. Higher period, low amplitude waves show greatest sensitivity to wind direction under stronger wind speeds, as local wind-generated waves are superimposed. The model highlights how different wind-wave conditions vary in the estuary, and stronger winds amplify and facilitate the propagation of long period, low amplitude further up-estuary under all conditions to impact infrastructure along the shoreline. The research helps to inform sea defense design to withstand wave overtopping under a range of conditions, minimize economic losses from operational downtime in ports and harbors due to wave transmission and inform long-term coastal management of the potential implications of future climate changes on wave hazard in the estuary. Future work needs to consider the effect of tide and surge on wave propagation, and results from fully coupled tide-surge-wind-wave models can force inundation models to explore depth and extent of flooding from severe storm events.

Declarations of interest

None.

Funding

This work was supported by the Engineering and Physical Sciences

Research Council as part of the Adaptation and Resilience of Coastal Energy Supply (ARCoES) project, grant number EP/I035390/1 and an EPSRC Impact Acceleration Account administered through the University of Liverpool. The research is also a contribution to UK NERC BLUEcoast Project (NE/N015924/1).

Acknowledgements

The authors thank colleagues at the British Oceanographic Data Centre (BODC) for providing tidal data; Magnox for providing tidal data; Environment Agency for providing tidal data; Gloucester Harbor Trustees for providing tidal data; UK Met Office for providing observational wind data; CEFAS for providing observational wave buoy data; EDINA for providing bathymetric data; and Judith Wolf at the National Oceanography Centre Liverpool for constructive comments on analysis of the wave buoy record.

References

- Allen, J.R., Duffy, M., 1998. Temporal and spatial depositional patterns in the Severn Estuary, southwestern Britain: intertidal studies at spring-neap and seasonal scales, 1991–1993. *Mar. Geol.* 146, 147–171. [https://doi.org/10.1016/S0025-3227\(97\)00124-2](https://doi.org/10.1016/S0025-3227(97)00124-2).
- Allsop, W., Bruce, T., Pearson, J., Alderson, J., Pullen, T., 2003. Violent wave overtopping at the coast, when are we safe? In: *International Conference on Coastal Management*, pp. 54–69.
- Allsop, W., Bruce, T., Pearson, J., Besley, P., 2005. Wave overtopping at vertical and steep seawalls. *Marit. Eng.* 158, 103–114.
- Allsop, W., Bruce, T.O.M., Pullen, T.I.M., Van der Meer, J., 2008. Direct hazards from wave overtopping - the forgotten aspect of coastal flood risk assessment? In: *43rd Defra Flood and Coastal Management Conference*, pp. 1–11.
- Ancil, F., Donelan, M.A., 1996. Air-water momentum flux observations over shoaling waves. *J. Phys. Oceanogr.* 26, 1344–1353.
- Bastidas, L.A., Knighton, J., Kline, S.W., 2016. Parameter sensitivity and uncertainty analysis for a storm surge and wave model. *Nat. Hazards Earth Syst. Sci.* 16, 2195–2210. <https://doi.org/10.5194/nhess-16-2195-2016>.
- BBC, 2014. River Severn bursts banks at Minsterworth after bore. [online]. Available at: <https://www.bbc.co.uk/news/uk-england-gloucestershire-25588120>, Accessed date: 6 July 2018.
- Bocquet, F., Flowerdew, J., Hawkes, P., Pullen, T., Tozer, N., 2009. Coastal Flood Forecasting: Model Development and Evaluation Protecting and Improving the Environment in England and.
- Booij, N., Ris, R.C., Holthuijsen, L.H., 1999. A third-generation wave model for coastal regions 1. Model description and validation. *J. Geophys. Res.* 104, 7649–7666.
- Bouma, J.J., François, D., Schram, A., Verbeke, T., 2009. Assessing socio-economic impacts of wave overtopping: an institutional perspective. *Coast. Eng.* 56, 203–209. <https://doi.org/10.1016/j.coastaleng.2008.03.008>.
- Bristol Port Company, 2018. The Bristol Port Company today. [online]. Available at: <https://www.bristolport.co.uk/about-us/bristol-port-company-today>, Accessed date: 5 July 2018.
- Brown, J.M., Davies, A.G., 2010. Flood/ebb tidal asymmetry in a shallow sandy estuary and the impact on net sand transport. *Geomorphology* 114, 431–439. <https://doi.org/10.1016/j.geomorph.2009.08.006>.
- Brown, J.M., Wolf, J., 2009. Coupled wave and surge modelling for the eastern Irish Sea and implications for model wind-stress. *Cont. Shelf Res.* 29, 1329–1342. <https://doi.org/10.1016/j.csr.2009.03.004>.
- Brown, J.M., Souza, A.J., Wolf, J., 2010. An 11-year validation of wave-surge modelling in the Irish Sea, using a nested POLCOMS – WAM modelling system. *Ocean Model.* 33, 118–128. <https://doi.org/10.1016/j.ocemod.2009.12.006>.
- Brown, J.M., Yelland, M.J., Pascal, R.W., Pullen, T., Bell, P.S., Cardwell, C.L., Jones, D.S., Milliken, N.P., Prime, T.D., Shannon, G., Ludgate, J.H., Martin, A., Farrington, B., Gold, I., Bird, C., Mason, T., 2018. WireWall: a new approach to coastal wave hazard monitoring. In: *Protection 2018, 3rd International Conference on Protection against Overtopping, Grange-Over-Sands, UK*, pp. 1–7.
- Burcharth, H., Hughes, S., 2011. Part VI, design of coastal project elements. In: *U.S. Army Corps of Engineers (Ed.), Coastal Engineering Manual*, pp. 378.
- Centre for Environmental Data Analysis, 2018. Met Office Integrated Data Archive System (MIDAS) Land and Marine Surface Stations Data. [online] Available at: <http://catalogue.ceda.ac.uk/> [Accessed January 2018].
- CEFAS, 2018. WaveNet Data Download. [online] Available at: <http://wavenet.cefas.co.uk> [Accessed January 2018].
- Chen, Q., Wang, U., Zhao, H., Douglass, S.L., 2007. Prediction of storm surges and wind waves on coastal highways in hurricane-prone areas. *J. Coast. Res.* 23, 1304–1317.
- Davies, J., 1964. A morphogenetic approach to world shorelines. *Z. Geomorphol.* 8, 27–42.
- Davis, R.A., Hayes, M.O., 1984. What is a wave-dominated coast? *Mar. Geol.* 60, 313–329.
- Desplanque, C., Mossman, D.J., 1999. Storm tides of the Fundy. *Am. Geogr. Soc.* 89, 23–33.
- Desplanque, C., Mossman, D.J., 2004. Tides and their seminal impact on the geology,

- geography, history, and socio-economics of the Bay of Fundy, eastern Canada (part 1: preface-chapter 3). *Atl. Geol.* 40, 3–35.
- Dhoop, T., Mason, T., 2018. Spatial characteristics and duration of extreme wave events around the English coastline. *J. Mar. Sci. Eng.* 6. <https://doi.org/10.3390/jmse6010014>.
- Diab, H., Younes, R., Lafon, P., 2017. Survey of research on the optimal design of sea harbours. *Int. J. Nav. Archit. Ocean Eng.* 9, 460–472. <https://doi.org/10.1016/j.ijnaoe.2016.12.004>.
- Donelan, M.A., 1982. The dependence of the aerodynamic drag coefficient on wave parameters. In: *Proceedings of the First International Conference on the Meteorology and Air-Sea Interaction of the Coastal Zone*, The Hague, Netherlands. American Meteorological Society, pp. 381–387.
- Dongeren, A. Van, Jong, M. De, Lem, C. Van Der, Deyzen, A. Van, den Bieman, J., 2016. Review of long wave dynamics over reefs and into ports with implication for port operations. *J. Mar. Sci. Eng.* 4, 1–10. <https://doi.org/10.3390/jmse4010012>.
- Dyer, K.R., 1995. Sediment transport processes in estuaries. In: *Geomorphology and Sedimentology of Estuaries*. Developments in Sedimentology, pp. 423–449. <https://doi.org/10.1007/978-1-61779-582-4>.
- Elias, E.P.L., Gelfenbaum, G., Westhuysen, A.J. Van Der, 2012. Validation of a coupled wave-flow model in a high-energy setting: the mouth of the Columbia River. *J. Geophys. Res.* 117, 1–21. <https://doi.org/10.1029/2012JC008105>.
- EurOtop, 2016. *Manual on Wave Overtopping of Sea Defences and Related Structures*.
- Fairley, I., Ahmadian, R., Falconer, R.A., Willis, M.R., Masters, I., 2014. The effects of a severn barrage on wave conditions in the Bristol Channel. *Renew. Energy* 68, 428–442. <https://doi.org/10.1016/j.renene.2014.02.023>.
- Geeraerts, J., Troch, P., Rouck, J. De, Verhaeghe, H., Bouma, J.J., 2007. Wave overtopping at coastal structures: prediction tools and related hazard analysis. *J. Clean. Prod.* 15, 1514–1521. <https://doi.org/10.1016/j.jclepro.2006.07.050>.
- Grady, J.G.O., McInnes, K.L., 2010. Wind waves and their relationship to storm surges in northeastern Bass Strait. *Aust. Meteorol. Oceanogr. J.* 60, 265–275.
- Greenberg, D.A., 1984. A review of the physical Oceanography of the Bay of Fundy. In: Gordon, D., Dadswell, M. (Eds.), *Update of the Marine Environmental Consequences of Tidal Power Development in the Upper Reaches of the Bay of Fundy*, pp. 9–30.
- Greenberg, D.A., Blanchard, W., Smith, B., Barrow, E., 2012. Climate change, mean sea level and high tides in the Bay of Fundy. *Atmos.-Ocean* 50, 261–276. <https://doi.org/10.1080/07055900.2012.668670>.
- Gridded bathymetry 1 Arcsecond [ascii], Scale 1:50,000, Tile: NW 55050025, NW 55050030, NW 55050035, NW 55050040, NW 55050045, NW 55100030, NW 55100035, NW 55100040, NW 55100045, NW 55150025, NW 55150030, NW 55150035, NW 55150040, NW 55150045, Updated August 2013. Crown Copyright/SeaZone Solutions Ltd., UK. Using: EDINA Marine Digimap Service. <http://edina.ac.uk/digimap> [Accessed January 2016].
- Haigh, I.D., Nicholls, R.J., 2017. Coastal flooding, marine climate change impacts partnership: science review. <https://doi.org/10.14465/2017.arci0.009-cof>.
- Haigh, I.D., Wadey, M.P., Gallop, S.L., Loehr, H., Nicholls, R.J., Horsburgh, K., Brown, J.M., Bradshaw, E., 2015. A user-friendly database of coastal flooding in the United Kingdom from 1915–2014. *Sci. Data* 2, 1–13. <https://doi.org/10.1038/sdata.2015.21>.
- Hoeke, R.K., McInnes, K.L., Grady, J.G.O., 2015. Wind and wave setup contributions to extreme sea levels at a tropical high island: a stochastic Cyclone simulation study for apia. Samoa. *J. Mar. Sci. Eng.* 3, 1117–1135. <https://doi.org/10.3390/jmse3031117>.
- Hu, K., Ding, P., Ge, J., 2007. Modeling of storm surge in the coastal waters of Yangtze estuary and Hangzhou Bay, China. *J. Coast. Res.* SI50, 527–533.
- Delft Hydraulics, 2014. *Delft3D-WAVE. Simulations of Short Crested Waves with SWAN Version 3.05, Revision 34160*. Deltarae, 2600 MH Delft, The Netherlands.
- Janssen, P.A.E.M., 1989. Wave-induced stress and the drag of air flow over sea waves. *J. Phys. Oceanogr.* 19, 745–754.
- Lesser, G.R., 2009. *An Approach to Medium-Term Coastal Morphological Modelling*.
- Lesser, G.R., Roelvink, J.A., van Kester, J.A.T.M., Stelling, G.S., 2004. Development and validation of a three-dimensional morphological model. *Coast. Eng.* 51, 883–915. <https://doi.org/10.1016/j.coastaleng.2004.07.014>.
- Letchford, C.W., Zachry, B.C., 2009. On wind, waves, and surface drag. In: *5th European & African Conferences on Wind Engineering*.
- Lin, W., Sanford, L.P., Suttles, S.E., Valigura, R., 2002. Drag coefficients with fetch-limited wind waves. *J. Phys. Oceanogr.* 32, 3058–3074.
- Liu, K., Chen, Q., Kalhatu, J.M., 2015. Modeling Wind Effects on Shallow Water Waves. *Journal of Waterway, Port, Coastal, and Ocean Engineering* 142 (1).
- Lyddon, C., Brown, J.M., Leonard, N., Plater, A.J., 2018a. Flood hazard assessment for a hyper-tidal estuary as a function of tide-surge-morphology interaction. *Estuar. Coasts* 41, 1–22. <https://doi.org/10.1007/s12237-018-0384-9>.
- Lyddon, C., Brown, J.M., Leonard, N., Plater, A.J., 2018b. Uncertainty in estuarine extreme water level predictions due to surge-tide interaction. *PLoS One* 13, 1–17.
- Magnox, 2014. *Hinkley Point A Site. Strategic Environmental Assessment Site Specific Baseline*.
- Masselink, G., Castelle, B., Scott, T., Dodet, G., Suarez, S., Jackson, D., Floe, F., 2016. Extreme wave activity during 2013/2014 winter and morphological impacts along the Atlantic coast of Europe. *Geophys. Res. Lett.* 43, 2135–2143. <https://doi.org/10.1002/2015GL067492>. Received.
- Monbaliu, J., Chen, Z., Felts, D., Ge, J., Hissel, F., Kappenberg, J., Narayan, S., Nicholls, R.J., Ohle, N., Schuster, D., Sothmann, J., Willems, P., 2014. Risk assessment of estuaries under climate change: lessons from Western Europe. *Coast. Eng.* 87, 32–49. <https://doi.org/10.1016/j.coastaleng.2014.01.001>.
- Natural Resources Wales, 2014. *Wales Coastal Flooding Review Phase 1 Report –Assessment of Impacts*.
- National Tidal and Sea Level Facility, 2018. *UK Tide Gauge Network*. [online] Available at: <http://www.ntsfl.org.uk/data/uk-network-real-time> [Accessed January 2018].
- Palmer, T., Nicholls, R.J., Wells, N.C., Saulter, A., Mason, T., 2014. Identification of “energetic” swell waves in a tidal strait. *Cont. Shelf Res.* 88, 203–215. <https://doi.org/10.1016/j.csr.2014.08.004>.
- Peel Ports, 2018. *History*. [online]. Available at: <https://www.peelports.com/about/history>, Accessed date: 5 July 2018.
- Phillips, M.R., 2008. Consequences of short-term changes in coastal processes: a case study. *Earth Surf. Process. Landforms* 2107, 2094–2107. <https://doi.org/10.1002/esp>.
- Phillips, M.R., Rees, E.F., Thomas, T., 2013. Winds, sea levels and North Atlantic Oscillation (NAO) in fl uences: an evaluation. *Glob. Planet. Chang.* 100, 145–152. <https://doi.org/10.1016/j.gloplacha.2012.10.011>.
- Phillips, B.T., Brown, J.M., Bidlot, J., Plater, A.J., 2017. Role of beach morphology in wave overtopping hazard assessment. *J. Mar. Sci. Eng.* 5, 1–18. <https://doi.org/10.3390/jmse5010001>.
- Prime, T., Brown, J.M., Plater, A.J., 2015. Physical and economic impacts of sea-level rise and low probability flooding events on coastal communities. *PLoS One* 10, 1–28. <https://doi.org/10.1371/journal.pone.0117030>.
- Prime, T., Brown, J.M., Plater, A.J., 2016. Flood inundation uncertainty: the case of a 0.5% annual probability flood event. *Environ. Sci. Policy* 59, 1–9. <https://doi.org/10.1016/j.envsci.2016.01.018>.
- Proctor, R., Flather, R.A., 1989. *Storm surge prediction in the Bristol Channel - the floods of 13 december 1981*. *Cont. Shelf Res.* 9, 889–918.
- Pugh, D.T., 2004. *Changing Sea Levels: Effects of Tides, Weather and Climate*. Cambridge University Press, Cambridge.
- Pye, K., Blott, S.J., 2010. A consideration of “extreme events” at Hinkley Point. *Technical Rep. Ser.* 2010.
- Pye, K., Blott, S.J., 2014. The geomorphology of UK estuaries: the role of geological controls, antecedent conditions and human activities. *Estuar. Coast Shelf Sci.* 150, 196–214. <https://doi.org/10.1016/j.ejss.2014.05.014>.
- Robins, P.E., Skov, M.W., Lewis, M.J., Giménez, L., Davies, A.G., Malham, S.K., Neill, S.P., McDonald, J.E., Whitton, T.A., Jackson, S.E., Jago, C.F., 2016. Impact of climate change on UK estuaries: a review of past trends and potential projections. *Estuar. Coast Shelf Sci.* 169, 119–135. <https://doi.org/10.1016/j.ejss.2015.12.016>.
- Rosa-Santos, P.J., Taveira-Pinto, F., 2013. Experimental study of solutions to reduce downtime problems in ocean facing ports: the Port of Leixões, Portugal, case study. *J. Appl. Water Eng. Res.* 1, 80–90. <https://doi.org/10.1080/23249676.2013.831590>.
- Santana-Ceballos, J., Fortres, C., Reis, M., Rodriguez, G., 2017. Wave overtopping and flood risk assessment in harbours: a case study of the Port of Las Nieves, Gran Canaria. *WIT Trans. Built Environ. Coast. Cities their Sustain. Futur.* II 170, 1–10. <https://doi.org/10.2495/CC170011>.
- Sibley, A., Cox, D., 2014. Flooding along English Channel coast due to long-period swell waves. *Weather* 69, 59–66.
- Sibley, A., Cox, D., Titley, H., 2015. Coastal flooding in England and Wales from atlantic and north sea storms during the 2013/2014 winter. *Weather* 70, 62–70.
- Stockdon, H.F., Holman, R.A., Howd, P.A., Sallenger Jr., A.H., 2006. Empirical parameterization of setup, swash, and runup. *Coast. Eng.* 53, 573–588. <https://doi.org/10.1016/j.coastaleng.2005.12.005>.
- Talke, S.A., Stacey, M.T., 2003. The influence of oceanic swell on flows over an estuarine intertidal mudflat in San Francisco Bay. *Estuar. Coast Shelf Sci.* 58, 541–554. [https://doi.org/10.1016/S0272-7714\(03\)00132-X](https://doi.org/10.1016/S0272-7714(03)00132-X).
- Thompson, D.A., Karunaratna, H., Reeve, D.E., 2017. Modelling extreme wave overtopping at Aberystwyth promenade. *Water* 9, 1–16. <https://doi.org/10.3390/w9090663>.
- Uncles, R.J., 2010. Physical properties and processes in the Bristol Channel and severn estuary. *Mar. Pollut. Bull.* 61, 5–20. <https://doi.org/10.1016/j.marpolbul.2009.12.010>.
- Van Deyzen, A.F.J., Beimers, P.B., Van Der Lem, J.C., Messiter, D., De Bont, J.A.M., 2015. To improve the efficiency of ports exposed to swell. In: *Australasian Coasts & Ports Conference 2015: 22nd Australasian Coastal and Ocean Engineering Conference and the 15th Australasian Port and Harbour Conference*.
- Welsh Office, 1999. *Coastal Survey - Wales: 1998 Snapshot*. Available at: <http://discovery.nationalarchives.gov.uk/details/r/C11525004>, Accessed date: 5 July 2018.
- Wolf, J., 2007. *Development of Estuary Morphological Models: Annex A1: SWAN Modelling of Liverpool Bay Including Dee, Mersey and Ribble Estuaries*. R&D Project Record FD2107/PR.
- Wolf, J., 2008. Coupled wave and surge modelling and implications for coastal flooding. *Adv. Geosci.* 17, 19–22.
- Wolf, J., 2009. Coastal flooding: impacts of coupled wave – surge – tide models. *Nat. Hazards* 49, 241–260. <https://doi.org/10.1007/s11069-008-9316-5>.
- Wolf, J., Brown, J.M., Bolaños, R., S, H.T., 2011. *Waves in Coastal and Estuarine Waters*, Treatise on Estuarine and Coastal Science. Elsevier Inc. <https://doi.org/10.1016/B978-0-12-374711-2.00203-5>.
- Woolf, D., Wolf, J., 2013. Impacts of Climate Change on Storms and Waves, *Marine Climate Change Impacts Partnership: Science Review*. <https://doi.org/10.14465/2013.arc03.020-026>.
- Wu, J., 1982. Wind-stress coefficients over sea surface from breeze to hurricane. *J. Geophys. Res.* 87, 9704–9706.
- Yap, W.Y., Lam, J.S.L., 2013. 80 million-twenty-foot-equivalent-unit container port? Sustainability issues in port and coastal development. *Ocean Coast Manag.* 71, 13–25.
- Yin, K., Xu, S., Huang, W., Xie, Y., 2017. Effects of sea level rise and typhoon intensity on storm surge and waves in Pearl River Estuary. *Ocean Eng.* 136, 80–93. <https://doi.org/10.1016/j.oceaneng.2017.03.016>.
- Zhang, J., Zhang, C., Wu, X., Guo, Y., 2012. Astronomical tide and typhoon-induced storm surge in Hangzhou Bay, China. In: Schulz, H.E., Simoes, A.L.A., Lobosco, R.J. (Eds.), *Hydrodynamics - Natural Water Bodies*. InTech. <https://doi.org/10.5772/28153>.